Light charged clusters emitted in 32 MeV/nucleon ^{136,124}Xe + ^{124,112}Sn reactions: Chemical equilibrium and production of ^{3}He and ^{6}He

R. Bougault,[1,*] E. Bonnet,[2] B. Borderie,[3] A. Chbihi,[4] D. Dell'Aquila,[3,5] Q. Fable,[4] L. Francalanza,[5] J. D. Frankland,[4] E. Galichet,[3,6] D. Gruyer,[7] D. Guinet,[8] M. Henri,[1] M. La Commara,[5] N. Le Neindre,[1] I. Lombardo,[5] O. Lopez,[1] L. Manduci,[9,1] P. Marini,[10] M. Pârlog,[1] R. Roy,[11] P. Saint-Onge,[11,4] G. Verde,[3,12] E. Vient,[1] and M. Vigilante[5]
(INDRA Collaboration)

[1]*Normandie Université, ENSICAEN, UNICAEN, CNRS/IN2P3, LPC Caen, F-14000 Caen, France*
[2]*SUBATECH UMR 6457, IMT Atlantique, Université de Nantes, CNRS-IN2P3, 44300 Nantes, France*
[3]*Institut de Physique Nucléaire, CNRS/IN2P3, Université Paris-Sud, Université Paris-Saclay, F-91406 Orsay cedex, France*
[4]*Grand Accélérateur National d'Ions Lourds (GANIL), CEA/DRFCNRS/IN2P3, Bvd. Henri Becquerel, 14076 Caen, France*
[5]*Dipartimento di Fisica 'E. Pancini' and Sezione INFN, Universitá di Napoli 'Federico II', I-80126 Napoli, Italy*
[6]*Conservatoire National des Arts et Metiers, F-75141 Paris Cedex 03, France*
[7]*Dipartimento di Fisica, Universitá di Firenze, via G. Sansone 1, I-50019 Sesto Fiorentino (FI), Italy*
[8]*IPNL/IN2P3 et Université de Lyon/Université Claude Bernard Lyon 1, 43 Bd du 11 novembre 1918, F-69622 Villeurbanne Cedex, France*
[9]*Ecole des Applications Militaires de l'Energie Atomique, BP 19 50115, Cherbourg Armées, France*
[10]*CEA, DAM, DIF, F-91297 Arpajon, France*
[11]*Laboratoire de Physique Nucléaire, Université Laval, Québec, Canada G1K 7P4*
[12]*INFN - Sezione Catania, via Santa Sofia 64, 95123 Catania, Italy*

(Received 13 March 2017; revised manuscript received 6 September 2017; published 20 February 2018)

Background: The isovector part of the nuclear equation of state remains partly unknown and is the subject of many studies. The degree of equilibration between the two main collision partners in heavy ion reactions may be used to study the equation of state since it is connected to isospin (N/Z) transport properties of nuclear matter.
Purpose: We aim to test chemical equilibrium attainment by measuring isotopic characteristics of emitted elements as a function of impact parameter.
Method: We study four ^{136,124}Xe + ^{124,112}Sn reactions at 32 MeV/nucleon. The data were acquired with the INDRA detector at the GANIL (Caen, France) facility. Combined (projectile+target) systems are identical for two studied reactions, therefore it is possible to study the path towards chemical equilibrium from different neutron to proton ratio (N/Z) entrance channels. The study is limited to identified isotopes detected in the forward part of the center of mass in order to focus on the evolution of projectile-like fragment isotopic content and the benefit of excellent detection performances of the forward part of the apparatus.
Results: Light charged particle productions, multiplicities, and abundance ratios dependence against impact parameter are studied. It is measured to almost identical mean characteristics for the two ^{124}Xe + ^{124}Sn and ^{136}Xe + ^{112}Sn systems for central collisions. Comparing all four studied systems it is shown that mean values evolve from projectile N/Z to projectile+target N/Z dependence. Those identical mean characteristics concern all light charged particles except ^{3}He whose mean behavior is strongly different.
Conclusions: Our inclusive analysis (no event selection) shows that N/Z equilibration between the projectile-like and the target-like is realized to a high degree for central collisions. The light charged particle production mean value difference between ^{124}Xe + ^{124}Sn and ^{136}Xe + ^{112}Sn systems for central collisions is of the order of a few %. This slight difference could be explained by pre-equilibrium particle emission whose intensity may differ for the two reactions. This point is demonstrated using ^{3}He mean characteristics whose production takes place before chemical equilibrium attainment. The realized N/Z balance between projectile-like and target-like does not imply a pure two-body mechanism. Indeed a midrapidity production of light charged particle does exist and its N/Z is different as compared to the projectile-like one: it is n enriched. This point is touched using ^{6}He midrapidity production which is favored by the drift phenomenon.

DOI: 10.1103/PhysRevC.97.024612

I. INTRODUCTION

The motivation for colliding nuclei at sufficient energy is to understand transport properties of nuclear matter and also study nuclear matter under extreme conditions [1]. These are

*Corresponding author: bougault@lpccaen.in2p3.fr

the two inseparable faces of heavy-ion reaction research which are related to dynamical and statistical physics.

The knowledge concerning the degree of equilibration between the two main collision partners is connected to both aspects, and many degrees of freedom are concerned with equilibration. At low bombarding energy [2] it has been shown that the N/Z ratio, isospin, is the fastest to be equilibrated. At higher bombarding energy, few tens MeV/nucleon, chemical equilibrium is driven by isospin diffusion in the presence of an isospin gradient between the projectile and the target [3] and by isospin drift sparked by a density gradient which occurs when a low density contact zone is created between the two partners [4]. The degree of chemical equilibration which is the N/Z balance between the projectile-like and the target-like is thus correlated to the interaction time between the two reaction partners, i.e., the time left to isospin drift and diffusion mechanisms to be fully efficient. In recent years many studies have been published concerning isospin transport in heavy ion reactions because it is connected to the knowledge of the isovector part of the equation of state and essential to resolve several issues in astrophysics (see [5] and references therein).

Our experimental analysis concerning isospin equilibrium may be compared with results obtained with symmetric systems at comparable bombarding energy [6,7]. We have here followed a different approach which is based on direct and simple observations: the presented analysis does not contain any data selection and presents mean value behaviors against reaction centrality.

II. EXPERIMENTAL DETAILS

The 4π multidetector INDRA [8] was used to study four reactions with beams of ^{136}Xe and ^{124}Xe, accelerated at 32 MeV/nucleon, and thin (530 μg/cm^2) targets of ^{124}Sn and ^{112}Sn. INDRA is a charged product multidetector, composed of 336 detection cells arranged in 17 rings centered on the beam axis and covering 90% of the solid angle. The first ring (2° to 3°) is made of 12 telescopes composed of 300 μm silicon wafer (Si) and CsI(Tl) scintillator (14 cm thick). Rings 2 to 9 (3° to 45°) are composed of 12 or 24 three-member detection telescopes: a 5 cm thick ionization chamber (IC), a 300 μm or 150 μm silicon wafer, and a CsI(Tl) scintillator (14 to 10 cm thick) coupled to a photomultiplier tube. Rings 10 to 17 (45° to 176°) are composed of 24, 16, or eight two-member telescopes: an ionization chamber and a CsI(Tl) scintillator of 8, 6, or 5 cm thickness. Indra can identify in charge fragments from hydrogen to uranium and in mass light fragments with low thresholds. Recorded event functionality was activated under a triggering factor based on a minimum number of fired detectors ($M^{\min}_{\text{trigger}}$) over the detector acceptance (90% of 4π). During the experiment, performed at GANIL (Caen, France), minimum bias ($M^{\min}_{\text{trigger}} = 1$) and exclusive ($M^{\min}_{\text{trigger}} = 4$) data were recorded.

The analysis is restricted to hydrogen and helium characteristics for which excellent mass and charge identification performances are achieved [8]. Two types of thresholds for H and He elements are used in this study: (i) for individual isotope characteristics, as multiplicities, only fully identified particles (A and Z) are taken into account, (ii) for global light charged particle variables, as light charged particle total transverse energy, solely Z identified particles are also included. For solely Z identified particles, $A = 1, 4$ is respectively assigned to all H, He elements and this increases by about 4%, 3%, respectively, the studied ^{1}H, ^{4}He populations as compared to the fully identified one.

This study is limited to the forward part of the center of mass (hereinafter called c.m.) and all figures, tables, and measured quantities are related to this half-hemisphere. It is thus focused on the evolution of projectile-like fragment isotopic content for which the INDRA multidetector, for these reactions, possesses excellent detection performances. The two studied reactions (^{124}Xe + ^{124}Sn and ^{136}Xe + ^{112}Sn) were chosen to study the path towards chemical equilibrium since their projectile+target combined systems are identical.

TABLE I. Detected reaction cross-section and corresponding maximum impact parameter for each studied reaction. Last column corresponds to detected cross-section values relative to predictions of [9]. Errors given in parenthesis are based on number of counts. The minimum bias samples were used.

	Detected cross section (mb)	$b_{\max}$ (fm)	Detected cross section (%)
^{124}Xe + ^{112}Sn	3550 (±3) mb	10.6 (±0.04) fm	64%
^{124}Xe + ^{124}Sn	3870 (±4) mb	11.1 (±0.06) fm	67%
^{136}Xe + ^{112}Sn	4145 (±4) mb	11.5 (±0.05) fm	72%
^{136}Xe + ^{124}Sn	4500 (±6) mb	12.0 (±0.08) fm	74%

III. DETECTED CROSS-SECTIONS

For minimum bias trigger recorded events, the detected reaction cross section is given in Table I. The corresponding maximum impact parameter is also indicated for each studied reaction.

Events with no detected light charged particle (H and He isotopes, hereinafter called lcp) in the forward part of the center of mass were eliminated. This condition ensures the elimination of the elastic scattering process but excludes also very peripheral reactions which lead to solely neutron evaporation. Uncharged particles are not detected by the apparatus nevertheless measured values indicate that a large fraction of the reaction cross section has been recorded when compared to predictions of [9] (see Table I). n-rich systems are slightly better detected than n-poor systems. This is probably caused by a smaller effect of the beam pipe dead zone for n-rich systems since a very peripheral event of neutron emission tends to deflect excited projectile prior tp lcp evaporation.

Forward c.m. detected cross sections are given in Table II for each type of lcp. The total lcp cross-section values are presented in the last line for each system and they show an almost, within 6%, system independence while the chemistry of lcp production is largely system dependent. As a matter of fact, increasing the neutron richness of the combined projectile-target system, we notice the following points: (i) n-poor particle (^{1}H, ^{3}He) production decreases, (ii) ^{4}He production is not strongly sensitive to N/Z change and

TABLE II. Forward c.m. detected lcp cross -sections. Values are given for each studied reaction (124 + 112 refers to ^{124}Xe + ^{112}Sn, etc.) and each type of fully identified lcp. Last line corresponds to the sum of lcp cross sections for each system. Statistical errors are given in parenthesis. The minimum bias samples were used.

	124+112	124+124
^{1}H	7963 (±7) mb	7167 (±5) mb
^{2}H	2485 (±4) mb	2714 (±3) mb
^{3}H	1342 (±3) mb	1780 (±2) mb
^{3}He	572 (±2) mb	491 (±1) mb
^{4}He	6992 (±6) mb	7257 (±5) mb
^{6}He	109 (±1) mb	147 (±1) mb
Total	19463 (±23) mb	19556 (±17) mb
	136+112	136+124
^{1}H	6621 (±7) mb	6241 (±5) mb
^{2}H	2773 (±5) mb	3092 (±4) mb
^{3}H	1965 (±4) mb	2612 (±3) mb
^{3}He	416 (±2) mb	397 (±1) mb
^{4}He	7005 (±8) mb	7501 (±6) mb
^{6}He	163 (±1) mb	239 (±1) mb
Total	18943 (±27) mb	20083 (±20) mb

it becomes the most produced particle, (iii) ^{2}H production increases while almost an equal value is measured for the two identical combined-N/Z systems, (iv) n-rich particle (^{3}H, ^{6}He) production largely increases—the cross-section values are doubled. Thus changing projectile and target N/Z, isotope production cannot be summed up in solely neutron production differences and these chemical modifications are the basic scope of this study.

IV. IMPACT PARAMETER EVALUATOR AND MIXED SAMPLES

Forward c.m. light charged particle total transverse energy $[(\Sigma E_t)^{lcp}_{\text{fw c.m.}}]$ distributions are displayed in Fig. 1 for the four reactions under minimum bias triggering condition. For very low $(\Sigma E_t)^{lcp}_{\text{fw c.m.}}$ values, the cross section is system dependent (see Fig. 1,bottom). For a transverse energy greater than 60 MeV the ^{136}Xe + ^{112}Sn and ^{124}Xe + ^{124}Sn distributions are identical. The ^{124}Xe + ^{112}Sn distribution merges the two identical ones at 100 MeV and finally all distributions behave the same for values greater than 150 MeV. This reflects the behavior of particle production related to nucleon exchanges between the projectile and the target as a function of impact parameter and the $(\Sigma E_t)^{lcp}_{\text{fw c.m.}}$ observable has been used, in the following, as an impact parameter evaluator [10].

The relationship between $(\Sigma E_t)^{lcp}_{\text{fw c.m.}}$ and the reduced impact parameter is given in Fig. 2 using the technique of Ref. [11] with minimum bias trigger condition data. It is observed that the 150 MeV value of the lcp transverse energy from which all $(\Sigma E_t)^{lcp}_{\text{fw c.m.}}$ distributions are identical corresponds to a 0.3 reduced impact parameter value, thus central collision events.

Figures 3 and 4 present ^{2}H Galilean invariant velocity plots for different impact parameter evaluator gates from peripheral to central ^{124}Xe + ^{124}Sn collisions.

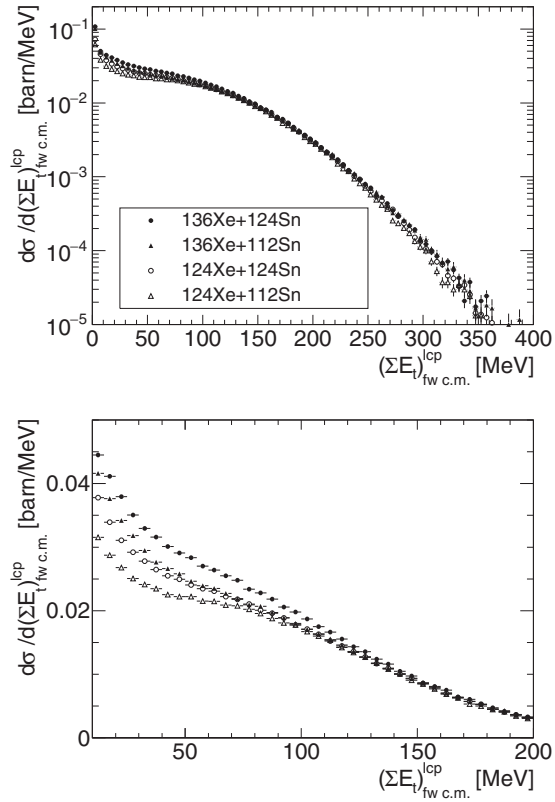

FIG. 1. Top: sum of light charged particle transverse energy distribution for the four studied reactions. Light charged particles refer to H and He isotopes detected in the forward part of the center of mass (minimum bias sample). Bottom: zoom of the left part of the top figure.

Emission from excited projectile-like fragment (PLF) is observed and is centered on a velocity value which evolves with impact parameter. This emission is increasing with the damping of the PLF velocity indicating an increase of the PLF excitation energy. The particle production whose velocity is located between the projectile-like and the target-like fragment (TLF) velocities is referred to as midrapidity production and it reflects the dynamical nature of the process which occurs between the two partners during the collision [12]. At this

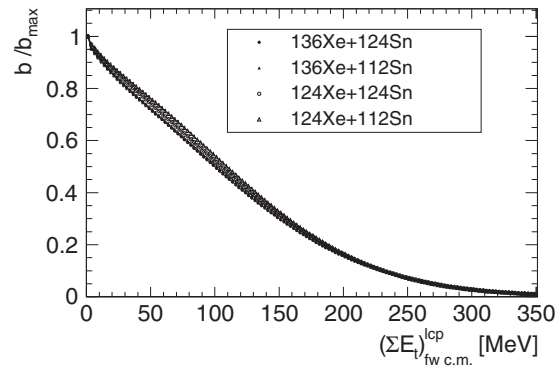

FIG. 2. Relationship between the impact parameter evaluator and the reduced impact parameter for the four studied reactions (minimum bias samples).

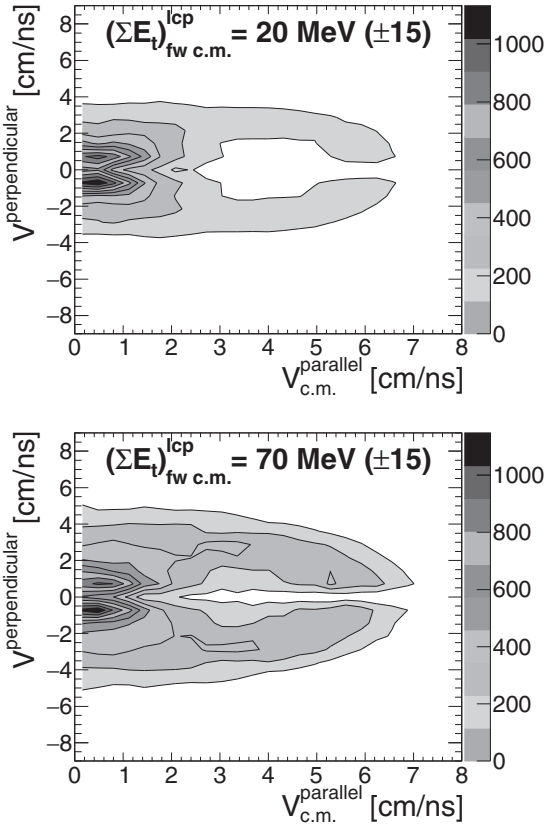

FIG. 3. ^{2}H Galilean invariant center of mass velocity contour plots for different impact parameter evaluator ranges (z scale: counts per cm^2/ns^2, bin size: 0.32×0.72 cm^2/ns^2). The ^{124}Xe + ^{124}Sn minimum bias sample was used.

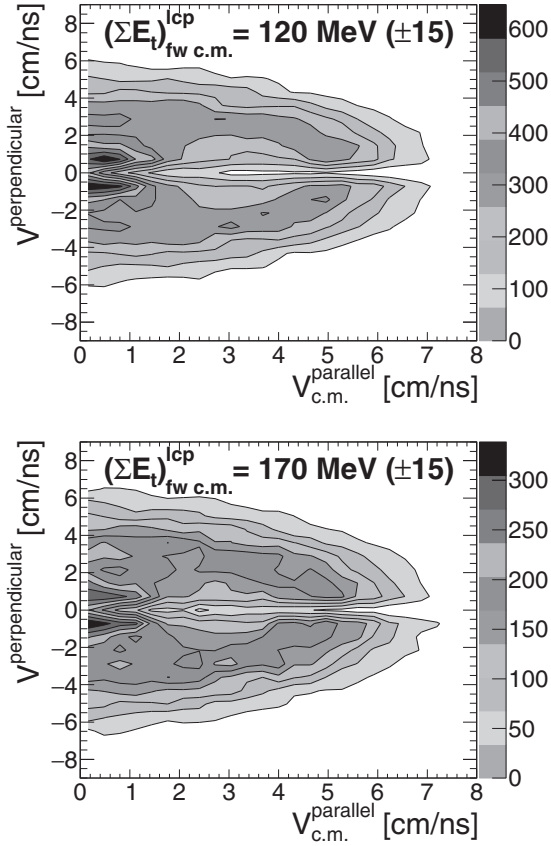

FIG. 4. ^{2}H Galilean invariant center of mass velocity contour plots for different impact parameter evaluator ranges (z scale: counts per cm^2/ns^2, bin size: 0.32×0.72 cm^2/ns^2). The ^{124}Xe + ^{124}Sn minimum bias sample was used.

bombarding energy the midrapidity region is populated by PLF and TLF emission and remnants of the contact region between the PLF and TLF where exchange of nucleons occurs between the two main partners. Midrapidity, or neck, has been evidenced in heavy-ion collisions ([12] and references therein) and was studied for Xe+Sn system at different bombarding energies [13]. Projectile/target nucleon exchange and midrapidity zone chemical composition is mainly governed by diffusion and drift isospin transport phenomena at this bombarding energy [3,4].

Figures 3 and 4 also indicate that when focusing on lcp production at different center of mass polar angle ranges, it is possible to approximately select projectile-like de-excitation (0°–30°) or midrapidity (60°–90°) populations. Whatever the lcp production mode (evaporation, simultaneous production, secondary decay, …) the global production is linked to the (neutron, proton) composition of the concerned angular zone and these angular selections will be used in the following for average behavior of both mentioned populations. More sophisticated selection methods exist for projectile-like de-excitation characterization but they only apply to very exclusive data [14].

A 4π multidetector is necessary to study reaction mechanisms but it implies a large flux of data during the experiment. This large flux generally causes large acquisition dead time. This issue is solved by reducing the beam intensity but longer run periods are necessary. A good compromise is to use exclusive data recording but one has to be able to verify that a correct sampling is achieved.

In our case most of the running period was done with $M^{\min}_{\text{trigger}} = 4$. A correct sampling check is done by applying, offline, the exclusive trigger condition to minimum bias trigger ($M^{\min}_{\text{trigger}} = 1$) recorded events and by comparing the selected impact parameter evaluator distribution to the original one. The sampling correctness is thus valued over the whole impact parameter range.

The ratio of the two distributions is presented in Fig. 5 for the four studied systems. It is seen that for $M^{\min}_{\text{trigger}} = 4$ condition, the level of eliminated events is kept below 3% for $(\Sigma E_t)^{lcp}_{\text{fw c.m.}}$ greater than 70 MeV for the four systems. Below this value the $M^{\min}_{\text{trigger}} = 4$ sampling depends on the impact parameter evaluator and is also system dependent. This implies studying very peripheral ($b/b_{\max}$ greater than about 0.7) events is not possible with $M^{\min}_{\text{trigger}} = 4$ running condition.

Most of the data taken was performed with the $M^{\min}_{\text{trigger}} = 4$ condition and thus for statistics purposes it may be convenient to mix inclusive and exclusive samples. A correct sampling ensemble is realized by mixing the $M^{\min}_{\text{trigger}} = 1$ sample for $(\Sigma E_t)^{lcp}_{\text{fw c.m.}}$ lower than 70 MeV and $M^{\min}_{\text{trigger}} = 4$ sample for $(\Sigma E_t)^{lcp}_{\text{fw c.m.}}$ greater than 70 MeV. In the following this mixed sample will be used when necessary.

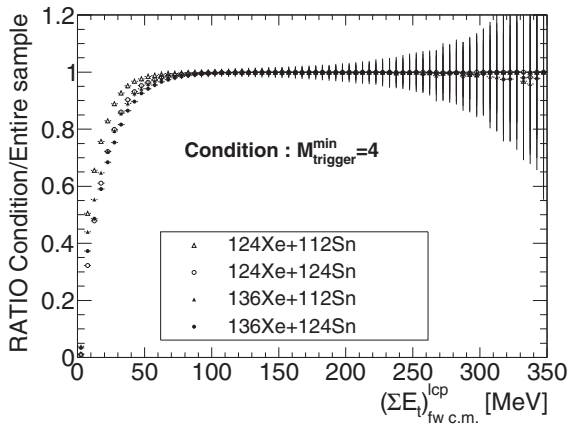

FIG. 5. Ratio between $(\Sigma E_t)^{lcp}_{\mathrm{fw\,c.m.}}$ distributions of $M^{\min}_{\mathrm{trigger}} = 4$ (off-line condition) and $M^{\min}_{\mathrm{trigger}} = 1$ for the four studied reactions. The minimum bias samples were used.

V. LIGHT CHARGED PARTICLE PRODUCTION

The forward center of mass lcp production is displayed in Fig. 6 for each studied system as a function of the impact parameter evaluator. For very peripheral collisions lcp production is largely dominated by ^{1}H production. ^{1}H production decreases and is partly replaced by cluster emission for smaller impact parameters while copious lcp production is achieved for more central collisions [$(\Sigma E_t)^{lcp}_{\mathrm{fw\,c.m.}}$ about 100 MeV]. This implies that global cross sections given in Table II are largely influenced by lcp production around 0.5 reduced impact parameter. The figure indicates three types of behavior against N/Z: (i) ^{3}He production is projectile dependent for almost all impact parameters, (ii) symmetric lcp (^{2}H and ^{4}He) production evolves from projectile dependence to system independence from peripheral to central reactions, (iii) n-rich lcp (^{3}H and ^{6}He) and ^{1}H productions evolve from projectile dependence to combined system dependence from peripheral to central reactions.

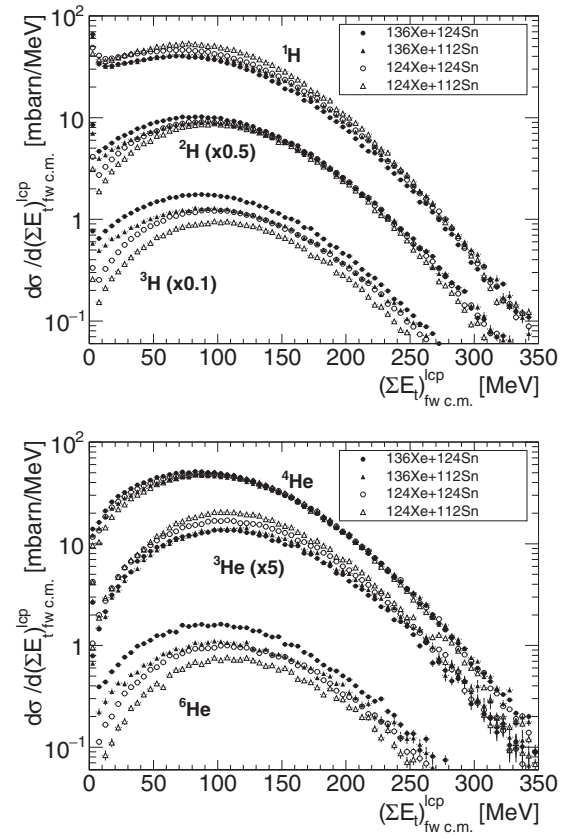

FIG. 6. Forward center of mass light charged isotope productions for each studied reaction as a function of the impact parameter evaluator (minimum bias samples).

Cross-section values reflect the production probabilities folded by the reaction cross section. Therefore those values cannot be used directly to study the chemical composition of the four exit channel reactions. Nevertheless from Fig. 1, identical ^{124}Xe + ^{124}Sn and ^{136}Xe + ^{112}Sn system reaction cross sections for $(\Sigma E_t)^{lcp}_{\mathrm{fw\,c.m.}} > 60$ MeV were noticed, whereas all studied system reaction cross sections are the same for $(\Sigma E_t)^{lcp}_{\mathrm{fw\,c.m.}} > 150$ MeV. This means that from a simple direct measurement, Fig. 6, it is possible to extract informations concerning N/Z equilibration selecting the forward part center of mass emitted lcp.

The lcp yields were presented in Fig. 6. The production probabilities, thus unfolded by the reaction cross section, are presented in Fig. 7 supplied as mean multiplicities relative to the impact parameter evaluator. It is seen that all mean multiplicities increase with decreasing impact parameter. Decreasing the impact parameter, the whole system is more and more excited and particle multiplicities increase. Because the impact parameter evaluator and lcp multiplicities are self-correlated, multiplicity increasing never ceases in Fig. 7. By comparing the values between the four systems it is possible to extract general evolutions. For very peripheral collisions, data are grouped in two categories (black points and white points, ^{136}Xe and ^{124}Xe projectiles, respectively). In that case, the multiplicity evolution depends on the nature of the projectile. Decreasing the impact parameter, particle production deviates from this first-order target independent behavior towards a dependence on the combined (projectile+target) system N/Z. This is evidenced by almost identical production, for central collisions, of most of the isotopes for the ^{124}Xe + ^{124}Sn and ^{136}Xe + ^{112}Sn systems. This evolution is visible because only forward c.m. lcp production is shown. For ^{2}H and ^{4}He, multiplicities evolve towards almost identical mean values for the four studied systems. ^{3}He multiplicity behavior is different since it presents a trend linked to memory of projectile N/Z for all impact parameters.

Figure 8 displays the ratios of mean multiplicities between the two identical global N/Z systems as a function of the impact parameter evaluator. The ratios present the evolution from peripheral to central events with the n-rich projectile system in the denominator. Thus n-rich particle ratios evolve from below unity towards unity values. This evolution is inverted for n-poor particle ratios while symmetric particle ratios do not present an identical evolution as a function of centrality. Except for ^{3}He, as previously stated, all ratios are close to unity for $(\Sigma E_t)^{lcp}_{\mathrm{fw\,c.m.}}$ greater than about 130 MeV.

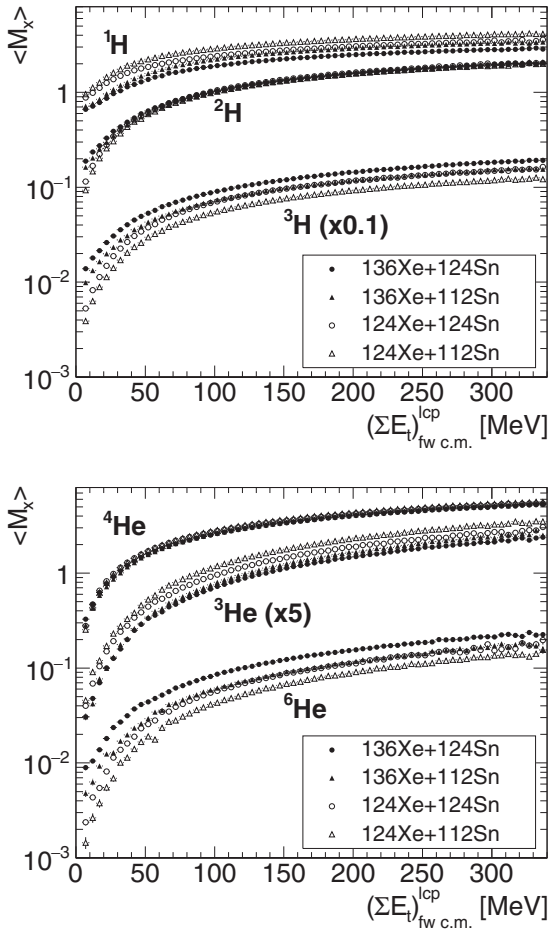

FIG. 7. Forward center of mass light charged isotope mean multiplicities for each studied reaction as a function of the impact parameter evaluator (mixed samples).

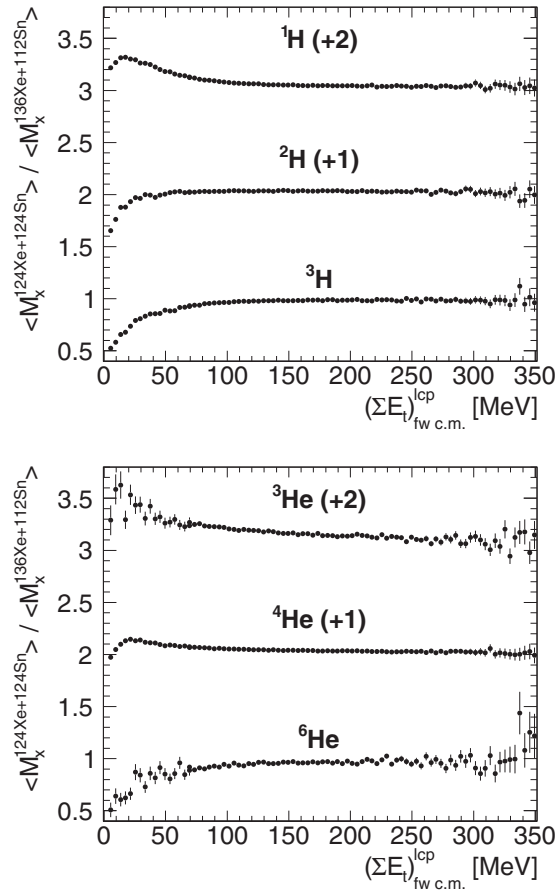

FIG. 8. Ratios of mean light charged isotope multiplicities between the ^{124}Xe + ^{124}Sn and ^{136}Xe + ^{112}Sn systems. In order to present the data in two pictures, a constant value (1 or 2) is added to certain ratios (mixed samples).

For very peripheral collisions the ^{1}H and ^{4}He ratios present a striking behavior since they first increase and then decrease with the impact parameter evaluator. In this study, peripheral reactions leading to only neutron production are excluded and therefore the mean lcp multiplicities of Fig. 7 are overestimated if that figure is interpreted as mean multiplicities versus impact parameter. Obviously this overestimation is dependant on the neutron richness of the projectile and not only ^{1}H and ^{4}He multiplicities are affected. Figure 7 is correct, only its representation in terms of impact parameter is not pertinent for $(\Sigma E_t)^{lcp}_{\mathrm{fw\,c.m.}}$ below about 30 MeV. Above this value, it is expected that all reaction processes produce at least one charged particle.

VI. CLUSTER ABUNDANCE RATIOS

In the previous section it was indicated that a mean multiplicity overestimation problem exists for very peripheral reactions if we think in terms of impact parameter dependence.

One way around this is to compare cluster mean multiplicities relative to proton mean multiplicity (hereafter called cluster abundance ratios [15]). Doing so, for each system the multiplicity overestimation seen for very peripheral collisions is canceled and it is then possible to compare cluster abundance ratios whatever the impact parameter is.

The use of cluster abundance ratios allows also to study the chemical equilibration process because trivial size dependences are removed [16]. In case of chemical equilibrium, one expects that both the ^{124}Xe + ^{124}Sn and ^{136}Xe + ^{112}Sn systems lead to the same cluster concentration for a given species so the same abundance ratio. ^{3}He characteristics will be studied in the next section because of their previously noticed peculiar behavior.

Cluster abundance ratios are presented in Figs. 9 and 10. Two center of mass lcp polar angular ranges are selected in order to approximately select projectile-like de-excitation (0°–30°) and midrapidity (60°–90°) populations. The ratios are calculated using the total number of clusters and proton detected in the given angular range and in the given impact parameter evaluator bin.

From the figures we conclude the following:

(i) Mean cluster abundance ratios are increasing with centrality. This implies an increase of composite particle production caused by an increase of excitation energy and nucleon-nucleon collisions.

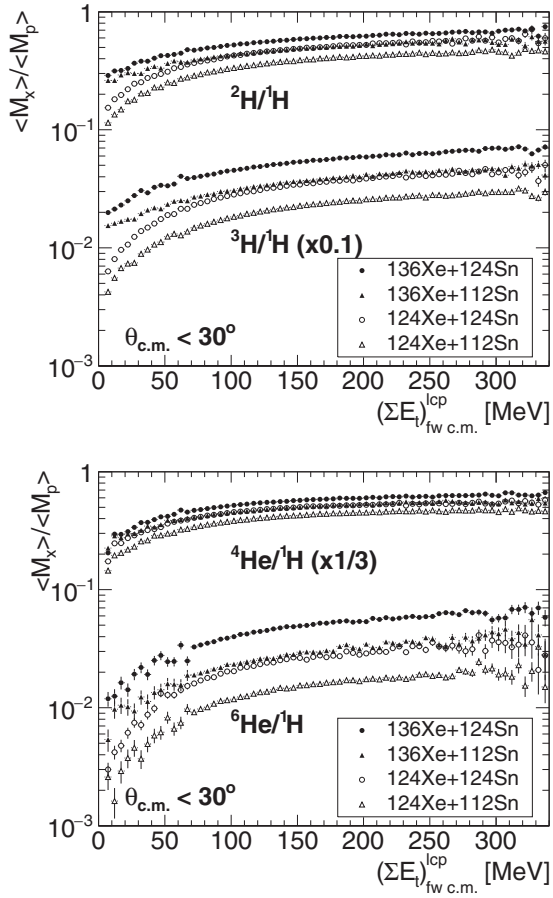

FIG. 9. Forward center of mass cluster abundance ratios for each studied reaction as a function of the impact parameter evaluator (mixed samples). Particles emitted forward (0°–30°).

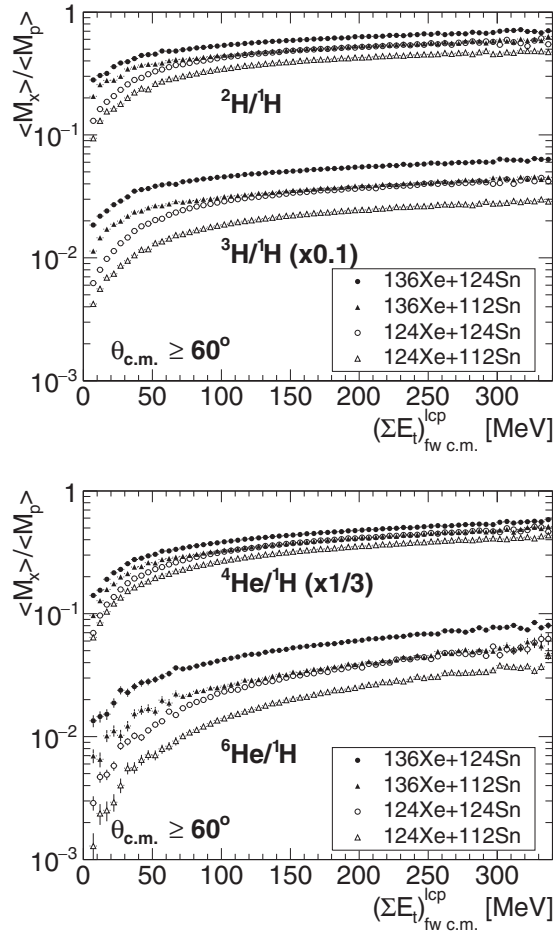

FIG. 10. Forward center of mass cluster abundance ratios for each studied reaction as a function of the impact parameter evaluator (mixed samples). Particles emitted perpendicular to the beam direction (60°–90°).

(ii) For $(\Sigma E_t)^{lcp}_{\text{fw c.m.}}$ greater than about 150 MeV, the ^{124}Xe + ^{124}Sn and ^{136}Xe + ^{112}Sn system mean abundance ratios are almost the same for a given cluster and a given angular range. This global N/Z system dependence implies that chemical equilibrium is almost realized for central collisions (reduced impact parameters lower about 0.3).

(iii) Cluster abundance ratio evolution against impact parameter evaluator reflects the dynamical process which occurs during the collision. For the projectile-like de-excitation region, the evolution starts from almost N/Z projectile dependence to N/Z total system dependence. For the midrapidity region the values are also projectile N/Z dependent for very peripheral reactions whereas they also reach a N/Z total system dependence for central collisions. This evolution reflects the drift/diffusion isospin phenomena and the midrapidity population behavior cannot be described by a pure participant/spectator scenario [17].

The two reactions ^{124}Xe + ^{124}Sn and ^{136}Xe + ^{112}Sn leading to the same projectile+target combined system were chosen to study the path towards chemical equilibrium. Comparing mean cluster abundance ratios we did not measure exactly the same values for the two systems. The original idea was neglecting pre-equilibrium particle emission which could be different for the two systems and thus explain the slight measured differences (few %). We will demonstrate this point in the next paragraph using ^{3}He production. Nevertheless the fact remains that measured cluster abundance ratio values between the two systems are so close, compared to the ^{124}Xe + ^{112}Sn and ^{136}Xe + ^{124}Sn systems, that the assumption of chemical equilibrium attainment is justified since abundance ratios are largely global (projectile+target) N/Z dependent.

VII. THE HELION CASE

The peculiar characteristic of ^{3}He, as compared to other lcp, produced in collisions between heavy targets with proton, light, or heavy projectiles has been pointed out in [16,18–21] and was previously indicated in this article.

Figures 11 and 12 show studied system mean helion multiplicities and abundance ratios for the two center of mass lcp polar angular ranges (projectile-like de-excitation and

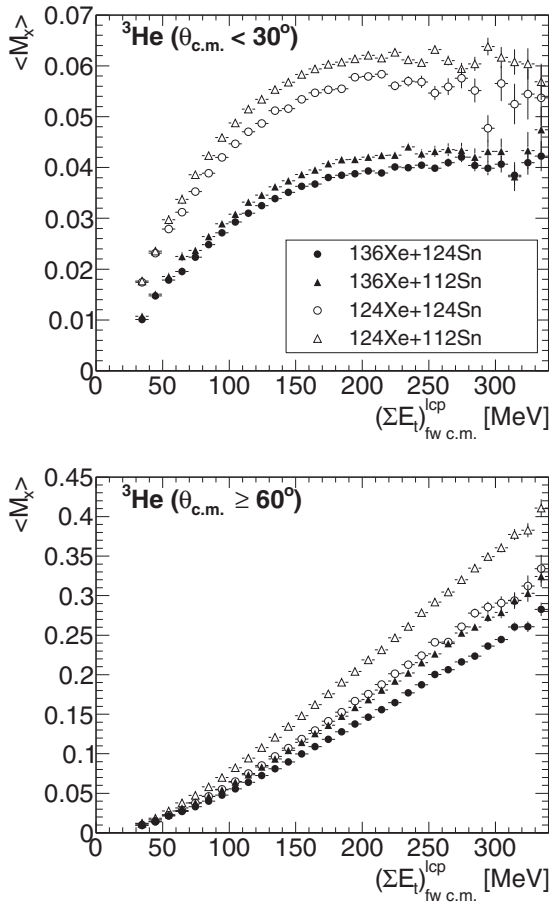

FIG. 11. Forward center of mass ^{3}He mean multiplicities for each studied reaction as a function of the impact parameter evaluator (mixed samples). Top: particles emitted forward (0°–30°). Bottom: particles emitted perpendicular to the beam direction (60°–90°).

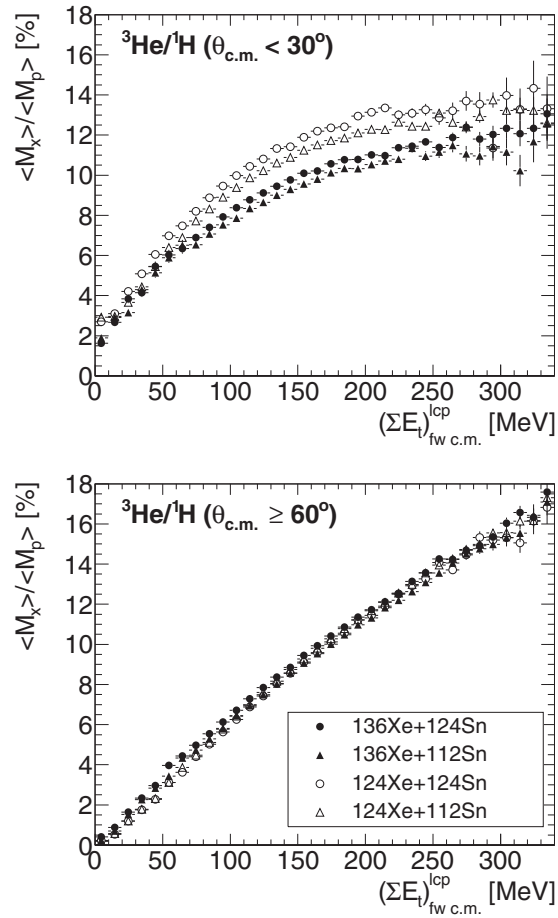

FIG. 12. Forward center of mass ^{3}He mean abundance ratios for each studied reaction as a function of the impact parameter evaluator (mixed samples). Abundance ratio values are in %. Top: particles emitted forward (0°–30°). Bottom: particles emitted perpendicular to the beam direction (60°–90°).

midrapidity populations) as a function of impact parameter evaluator. The figures show that helion production is very different as compared to other lcp presented in Figs. 9 and 10. First, for all impact parameters the behavior between 0°–30° and 60°–90° populations is not the same. Secondly, when comparing the different system productions it is also observed that:

(i) The mean multiplicities remain largely projectile-dependent for the projectile-like population while it is total system (projectile+target) dependent for the midrapidity population. This is true whatever the impact parameter is. In both cases an n-poor system favors helion production.

(ii) Looking at ^{3}He abundance ratios one observes that (i) projectile-like population remains largely projectile dependent for the whole impact parameter range, (ii) midrapidity population is independent of the reaction system for all impact parameters except to a certain extent for very peripheral collisions.

Putting together multiplicity and abundance ratio results, it is then observed that helion production conserves a footprint of initial projectile N/Z for the 0°–30° domain while it depends on the size (not N/Z) of the overlapping region between the projectile and the target for the 60°–90° domain.

Isospin diffusion and drift are driving the chemical equilibrium process. The latter phenomenon causes a neutron enrichment of the midrapidity zone ([22,23] and references therein) while the isospin diffusion tends to N/Z equilibrium between projectile and target collision partners. The observed results imply an average helion production prior chemical equilibrium attainment. For the case of the midrapidity region, the neutron enrichment which occurs for all studied reactions disadvantages helion production when it becomes efficient. Keeping in mind that mean values are studied, these observations do not imply that all helion are produced before drift and diffusion mechanisms become fully effective, they rather imply that helion production is strongly reduced when those mechanisms act.

The mean pre-equilibrium character of ^{3}He and its production difference between the studied systems for the 0°–30° domain would appear to explain the small measured abundance ratio differences between ^{124}Xe + ^{124}Sn and ^{136}Xe + ^{112}Sn

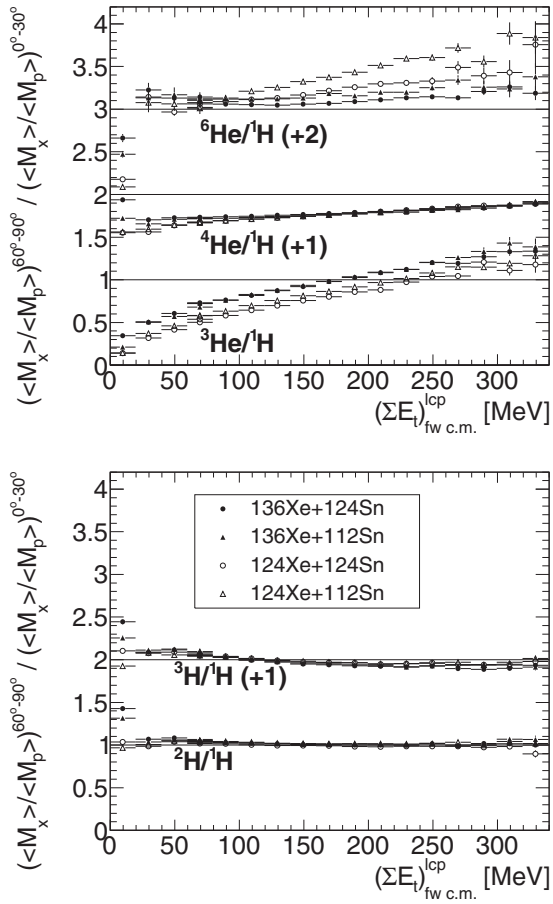

FIG. 13. Forward center of mass ^{2}H, ^{3}H, ^{3}He, ^{4}He, ^{6}He fractions for each studied reaction as a function of the impact parameter evaluator (mixed samples). lcp fractions are 60°–90° divided by 0°–30° lcp abundance ratios. In order to present the data in two pictures, a constant value (1 or 2) is added to certain fractions.

systems. Other lcp are certainly partly concerned by pre-equilibrium production which gives rise to transparency effect [24] but in average other lcp do not present this character.

VIII. MIDRAPIDITY NEUTRON ENRICHMENT AND THE ^{6}He CASE

Solid angle independence of cluster abundance ratios permits to compare directly the projectile-like and midrapidity mean values previously presented. The fraction between mean values of midrapidity and projectile-like angular regions against the impact parameter evaluator are presented in Fig. 13 for H and He isotopes.

(i) Concerning the system dependence, ^{3}He fraction values reflect the 0°–30° abundance ratio behavior since ^{3}He abundance ratios are system independent for the 60°–90° populations. It is not the case for the other particles.

(ii) ^{2}H, ^{3}H, and ^{4}He fractions are system independent for central collisions. Except for peripheral reactions, the ^{2}H fractions for the two populations (0°–30° and 60°–90°) are identical. To a certain extent this is also true for ^{3}H fractions. For ^{4}He fractions, some differences are observed at low $(\Sigma E_t)^{lcp}_{\text{fw c.m.}}$ values and the increasing behavior with impact parameter evaluator may reflect angular momentum effects since ^{4}He can remove appreciable angular momentum from the excited projectile-like.

(iii) ^{6}He fraction values are increasing with impact parameter evaluator as ^{4}He but ^{6}He fraction values are always larger than unity except for very peripheral collisions. This means that the midrapidity region favors very neutron rich cluster production whatever the impact parameter is. Concerning the system dependence, the figure indicates that the more n-poor the system is, the greater the fraction value.

Besides the ^{3}He pre-equilibrium nature, those observations imply two different mean particle production modes for all impact parameters: projectile-like de-excitation and midrapidity sources whose N/Z are different for a given system and a given impact parameter. ^{2}H and ^{3}H fraction values may imply that, in average, the projectile-like de-excitation process is largely dominating the production for reduced impact parameters below around 0.6. The drift phenomenon may explain the system dependence of ^{6}He fractions: the n-enrichment of the midrapidity source dries out the projectile-like from sufficient neutron concentration to produce very rich neutron clusters, the more n-poor the system is, the more dramatic is the effect. For the ^{124}Xe + ^{112}Sn reaction this cannot be counterbalanced by the diffusion effect since the projectile and target N/Z are similar.

IX. CONCLUSION

We have presented an analysis concerning INDRA multidetector data acquired through 32 MeV/nucleon ^{136,124}Xe + ^{124,112}Sn reactions. The study was restricted to the forward part of the center of mass emitted light charged particles because for those particles the excellent detection performance allows to carry out inclusive analysis. Two studied reactions (^{124}Xe + ^{124}Sn and ^{136}Xe + ^{112}Sn) were chosen to study the degree of chemical equilibrium, i.e., the N/Z balance between the projectile and the target. This balance was studied for all types of collisions by estimating the impact parameter. Shown results concern average behaviors and no event selection was performed (inclusive analysis).

Light charged particle productions, multiplicities, and abundance ratios dependence against impact parameter indicate that chemical equilibrium is realized in central collisions to a high degree. This conclusion was established by measuring almost identical mean characteristics for the two ^{124}Xe + ^{124}Sn and ^{136}Xe + ^{112}Sn systems for central collisions. Comparing all four studied systems impact parameter dependance it was shown that mean values evolve from projectile N/Z to projectile+target N/Z dependence.

This high degree of equilibration is of the order of few % difference for ^{124}Xe + ^{124}Sn and ^{136}Xe + ^{112}Sn systems. This slight difference could be explained by pre-equilibrium particle emission whose intensity may differ for the two reactions. This

point has been demonstrated using ^{3}He mean characteristics which strongly differ from other lcp behaviors. It has been shown that helion production takes place before chemical equilibrium attainment.

The realized N/Z balance between the projectile and target does not imply a pure two-body mechanism. Indeed a midrapidity production of lcp does exist and its N/Z is different as compared to the projectile-like one: it is n-enriched. This point has been touched using ^{6}He midrapidity production which is favored by the drift phenomenon.

Our results differ from those of [6] and [7]. We recall that here raw data are used while the cited results are extracted using reconstructing methods or obtained through a restricted rapidity region of the phase space.

With the advent of the wide range mass and charge identification FAZIA detector [25], this study could be extended to higher elements.

Finally we think that ^{6}He and ^{3}He productions may be used for comparing data to transport model results concerning the knowledge of the equation of state and its isospin dependence.

[1] *Dynamics and Thermodynamics with Nuclear Degrees of Freedom*, edited by P. Chomaz, F. Gulminelli, W. Trautman, and S. Yennello, in Eur. Phys. J. A **30**, thematic issue No. 1 (2006), pp. 1–342.

[2] J. Galin *et al.*, Z. Phys. A **278**, 347 (1976).

[3] T. X. Liu, W. G. Lynch, M. B. Tsang, X. D. Liu, R. Shomin, W. P. Tan, G. Verde, A. Wagner, H. F. Xi, H. S. Xu, B. Davin, Y. Larochelle, R. T. de Souza, R. J. Charity, and L. G. Sobotka, Phys. Rev. C **76**, 034603 (2007).

[4] V. Baran *et al.*, Phys. Rep. **410**, 335 (2005).

[5] *Topical Issue on Nuclear Symmetry Energy*, edited by B.-A. Li, A. Ramos, G. Verde, and I. Vidaña, in Eur. Phys. J. A **50**, topical issue No. 2 (2014), pp. 9–49.

[6] A. L. Keksis, L. W. May, G. A. Souliotis, M. Veselsky, S. Galanopoulos, Z. Kohley, D. V. Shetty, S. N. Soisson, B. C. Stein, R. Tripathi, S. Wuenschel, S. J. Yennello, and B. A. Li, Phys. Rev. C **81**, 054602 (2010).

[7] Z. Y. Sun, M. B. Tsang, W. G. Lynch, G. Verde, F. Amorini, L. Andronenko, M. Andronenko, G. Cardella, M. Chatterje, P. Danielewicz, E. DeFilippo, P. Dinh, E. Galichet, E. Geraci, H. Hua, E. LaGuidara, G. Lanzalone, H. Liu, F. Lu, S. Lukyanov, C. Maiolino, A. Pagano, S. Piantelli, M. Papa, S. Pirrone, G. Politi, F. Porto, F. Rizzo, P. Russotto, D. Santonocito, and Y. X. Zhang, Phys. Rev. C **82**, 051603(R) (2010).

[8] J. Pouthas *et al.*, Nucl. Instrum. Methods Phys. Res. A **357**, 418 (1995).

[9] S. Kox *et al.*, Nucl. Phys. A **420**, 162 (1984).

[10] V. Metivier *et al.*, Nucl. Phys. A **672**, 357 (2000).

[11] C. Cavata, M. Demoulins, J. Gosset, M.-C. Lemaire, D. L'Hôte, J. Poitou, and O. Valette, Phys. Rev. C **42**, 1760 (1990).

[12] M. Di Toro *et al.*, Eur. Phys. J. A **30**, 65 (2006).

[13] E. Plagnol *et al.* (The INDRA Collaboration), Phys. Rev. C **61**, 014606 (1999).

[14] E. Vient *et al.*, arXiv:1709.07396.

[15] H. Gutbrod *et al.*, Rep. Prog. Phys. **52**, 1267 (1989).

[16] W. Reisdorf *et al.*, Nucl. Phys. A **848**, 366 (2010).

[17] G. D. Westfall *et al.*, Phys. Rev. Lett. **37**, 1202 (1976).

[18] A. M. Poskanzer *et al.*, Phys. Rev. C **3**, 882 (1971).

[19] H. F. Xi, G. J. Kunde, O. Bjarki, C. K. Gelbke, R. C. Lemmon, W. G. Lynch, D. Magestro, R. Popescu, R. Shomin, M. B. Tsang, A. M. Vandermolen, G. D. Westfall, G. Imme, V. Maddalena, C. Nociforo, G. Raciti, G. Riccobene, F. P. Romano, A. Saija, C. Sfienti, S. Fritz, C. Gross, T. Odeh, C. Schwarz, A. Nadasen, D. Sisan, and K. A. G. Rao, Phys. Rev. C **58**, R2636(R) (1998).

[20] N. Marie *et al.*, Phys. Lett. B **391**, 15 (1997).

[21] W. Neubert *et al.*, Eur. Phys. J. A **7**, 101 (2000).

[22] Y. Larochelle *et al.*, Phys. Rev. C **62**, 051602(R) (2000).

[23] S. Barlini, S. Piantelli, G. Casini, P. R. Maurenzig, A. Olmi, M. Bini, S. Carboni, G. Pasquali, G. Poggi, A. A. Stefanini, R. Bougault, E. Bonnet, B. Borderie, A. Chbihi, J. D. Frankland, D. Gruyer, O. Lopez, N. LeNeindre, M. Parlog, M. F. Rivet, E. Vient, E. Rosato, G. Spadaccini, M. Vigilante, M. Bruno, T. Marchi, L. Morelli, M. Cinausero, M. Degerlier, F. Gramegna, T. Kozik, T. Twarog, R. Alba, C. Maiolino, and D. Santonocito (FAZIA Collaboration), Phys. Rev. C **87**, 054607 (2013).

[24] O. Lopez, D. Durand, G. Lehaut, B. Borderie, J. D. Frankland, M. F. Rivet, R. Bougault, A. Chbihi, E. Galichet, D. Guinet, M. La Commara, N. Le Neindre, I. Lombardo, L. Manduci, P. Marini, P. Napolitani, M. Pârlog, E. Rosato, G. Spadaccini, E. Vient, and M. Vigilante (INDRA Collaboration), Phys. Rev. C **90**, 064602 (2014).

[25] R. Bougault *et al.*, Eur. Phys. J. A **50**, 47 (2014).